Chapter 5

Fabrication of Conducting Nanochannels using Accelerator for Fuel cell Membrane and Removal of Radionuclides: Role of Nanoparticles

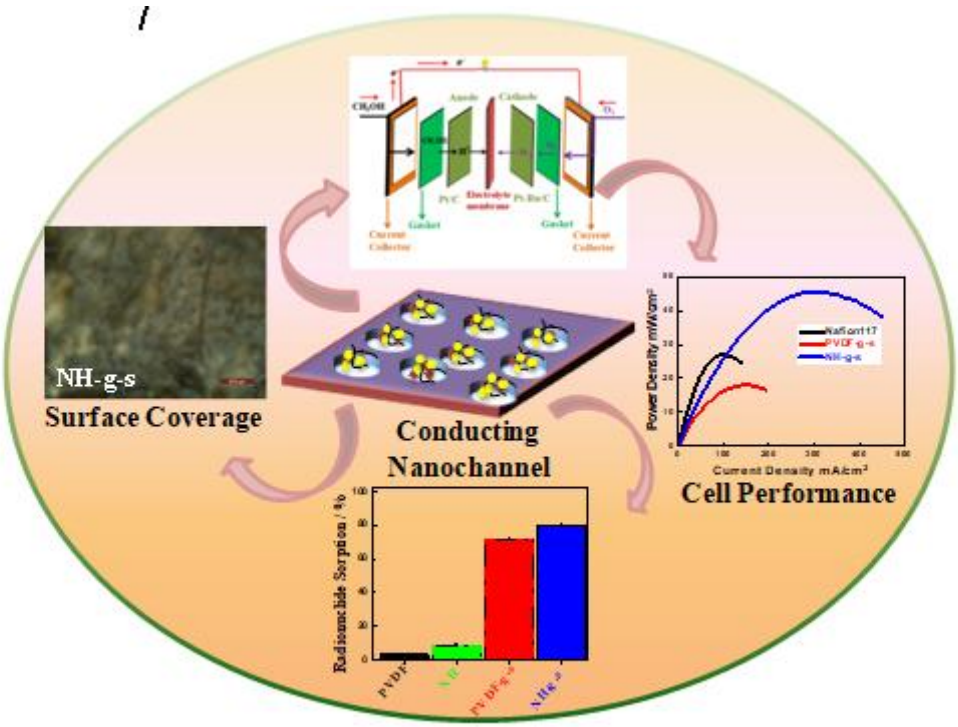

5.1 Introduction:

Polymeric membranes exhibit their better efficiency towards many industrial applications such as air purification, water filtration [9], sensor, ion transport and energy production using a greener technology [8], [9], [197]. Apart from these applications, separation technology is a fundamental aspect of the chemical industries and academic view point [198],[199]. Amongst the nature of separations, the radioactive waste treatment is of prime importance especially in nuclear power plants and health departments, specifically in the field of cancer cell imaging[25], [200], [201]. Recently, the separation and sensing of the radioactive sources from the aqueous/waste solution is of prime importance. Ion exchange membranes (IEM) have engage much attention as because of its is easily portable , ambient temperature operation , having light weight and high power density [202][203][204]. The membrane driven technologies provide clean and affordable source of energy for portable and stationary electronics. Recent developmental works are focusing on fuel cells as they are found to be suitable for the alternative of fossil fuels to avoid increasing environmental pollution [98][60]. The key component to figure out such kind of issue is the advancement of ion exchange membrane (IEM), which is the key component of any electrochemical system such as batteries, electrochemical sensor, fuel cell, solar cell including ion / charge carrier exchange/ transport phenomena [205][4]. The exchange and complexing tendency of the membrane are introduced through grafting of polymer backbone using different monomers followed by functionalization by means of ionic species, such as sulphates, phosphate, chlorides etc.,[206][97][207] best suitable for cationic and quaternary ammonium, phosphonium ions etc. as anionic membranes [208][209]. These ionic species also facilitate the transport/sorption of ions through the membrane [210]. These membranes

are used as electrolytes in fuel cell technology which work as the barrier for the electron and facilitate the transport of ions (Proton) from one side of the membrane to other side and separate the electron or ions by capturing the functional groups which either form complex with ions or exchange the ionic species.[23] Different methods are reported in the literature to introduce different functional groups in polymer chain such as chemical methods, UV radiation, γ-irradiation and swift heavy ions (SHI) bombardments etc.[66] Amongst these processes, high energy heavy ion bombardment is the most promising technique [66]. When irradiated on polymer films, the swift heavy ions lose maximum energy when pass through it thin polymeric film [170] The loss of energy occurs both due to atomic collision and electronic excitation/ionization when they interact with polymer molecules. [98] Moreover, the path of the latent tracks is predominantly amorphous in nature, which can be removed in a convenient way through selective chemical etching and finally creating through nanochannels across the depth of thin film. The channel shape and size depends upon the factors such as mass of ions, fluence of ions, linear energy transfer and etching conditions such as time and temperature. [211] After the irradiation followed by etching process, different physical as well as chemical changes occur in the polymer film such as bond breaking, new bond formation *e.g.* double bond formation, some by-product formation along with the creation of ionic species or free radical active sites which are eventually responsible for grafting followed by functionalization to induct ionic species.[158][172][8] High proton conductivity, low fuel cross over, sufficient water uptake with better thermal and mechanical properties along with cost and durability are the essential parameters for an efficient fuel cell membrane.[212] Ionomer Nafion117 is the commercial membrane which is developed by the DuPont Inc., [174] having its

disadvantages of high fuel cross over, poor thermal and ion conduction at high temperature.[175][114]

Fluoropolymers, such as poly(vinylidene fluoride) (PVDF) and its copolymers show excellent properties such as thermal, mechanical stability and durability along with their non reactive and insulating behavior [179][180] which make them suitable ionic membrane for the above applications. PVDF and its copolymers exist in five different phases broadly classified as polar and non-polar phases, polar or partial polar phases are β, γ, δ and ε and non polar phase is α with the added advantage that meta-stable polar phase, also piezoelectric, can be induced by the addition of some specific fillers.[152]

In this work, highly conducting nanochannel are fabricated using accelerator irradiation followed by their chemical etching, subsequent grafting of common monomer, followed by sulphonation of the grafted species within the nanochannel exclusively to convert them into ion conducting channels. The developed membranes are used for radio nuclide separation from the radioactive waste and to understand the mechanism of greater efficiency from the confinement effect. Further, membrane electrode assembly has been fabricated using the membrane and its efficiency in fuel cell has been tested and compared with standard commercial membrane. However, the membrane is effective both in terms of heavy metal removal including radio nuclides and is able to generate energy in a fuel cell without any trade off in an effective manner.

5.2 Experimental

5.2.1 Materials: PVDF, poly (vinylidene difluoride) SOLEF 11008 , 30B [bis (hydroxyethyl) methyl tallow ammonium ion exchanged montmorillonite, Potassium permanganate ($KMnO_4$) and sodium hydroxide (NaOH), ($K_2S_2O_5$) potassium meta-

bisulphate, styrene monomer, Chlorosulphonic acid (HSO_3Cl) , Nitric acid (HNO_3) , H_2SO_4. Preparation of the nanohybrid membrane is discussed in details in **chapter 2**.

5.2.2 Functionalization of the membrane:

Around 30 μm thin films of *PVDF* and its nanohybrid (*NH*) were irradiated by using 140 MeV Ag^+ ions in a vacuum of 5 $\times 10^{-6}$ mbar at the Inter University Accelerator Center, New Delhi, India. The ion fluence (number of ions per unit area) used was 1×10^7 ions/cm^2 to ensure that sufficient number of latent tracks are produced in the membrane. The Irradiation experiments were carried out in GPSC (general purpose scattering chamber) using a thin gold foil (250 μg/cm^2). The irradiated pristine *PVDF* and its nanohybrid (NH) films were chemically etched using potassium permanganate solution (0.25 mol /*L*) in a highly alkaline medium (9 mol/*L*) at 65 ^oC for 4 h. The etched films with brownish precipitate of MnO_2 were quickly immersed in a $K_2S_2O_5$ saturated solution for 30 min followed by washing in distilled water. The residual water at the surface was removed with a filter paper and was dried at 65 ^oC for 24 h in a vacuum oven under reduced pressure. The porous etched films (4×4 cm^2) were immersed in the monomer solution (4 ml distilled non-ionized form of styrene monomer in 16 ml distilled Toluene) to initiate the grafting process under nitrogen atmosphere. Solution containing the film was stirred (solution polymerization) at 0 ^oC for 24 h under nitrogen atmosphere. The homopolymer, styrene other than grafted was washed away after stirring in toluene for 12 h. Finally, the films were washed with methanol (CH_3OH) and were dried at 65 ^oC overnight under reduced pressure in vacuum oven. Sulphonation (electrophilic substitution reaction) has been performed on the styrene grafted *PVDF* and its *NH* films using chlorosulphonic (HSO_3Cl) acid at 65 ^oC for 30 min. The condition was optimized by altering the temperature and time

so that mechanically stable polymer films were obtained after chemical modification for ready to use in present application. The films were washed with deionized water after the sulphonation and were dried at 65 ^{o}C for 24 h under reduced pressure. The term PVDF-e or NH-e, and PVDF-g-s or NH-g-s refer to the etched and grafted followed by sulphonated membrane, respectively. The schematic of the irradiated membrane preparation, chemical etching followed by functionalization is shown in **Figure 5.1a** and the scheme of functionalization using monomer followed by sulphonation is shown in the **Figure 5.1b**.

5.4 Results and discussion:

5.3.1 Nanochannel fabrication using swift heavy ions:

Bombardment of charged particles, so called swift heavy ions, on the surface of polymeric film generates latent track in the path of the ions and the passages predominantly become amorphous in nature. These amorphous latent tracks are sensitive towards chemical etchant which selectively remove the amorphous track and thereby create through nanochannels in the film and subsequently expose the free radicals in the walls of the nanochannels .[106] The bombardment of high energy particle radiation (SHI) on Pristine PVDF and its nanohybrid membrane cause different chemical changes such as C-H, C-F or C-C bonds are breakage because of the SHI energy (~100 MeV) is very high in contrast to the bond dissociation energy of C-H, C-F and C-C bond energies of 4.4, 4.8 and 3.6 eV (per bond), respectively, due to lesser bond energy as compare to SHI energy, resulting in formation of the reactive site in the polymer such as Free radical , double bond, cross linking ,chain scission and latent track etc. [106] This is to mention that SHI irradiation generates reactive free radicals in polymer chains as the energy of SHI (~100 MeV) is much higher than that

of carbon-hydrogen or carbon-carbon bonds. Complete steps of the chemical changes and the nanochannel creation are shown schematically in **Figure 5.1(a & b).**

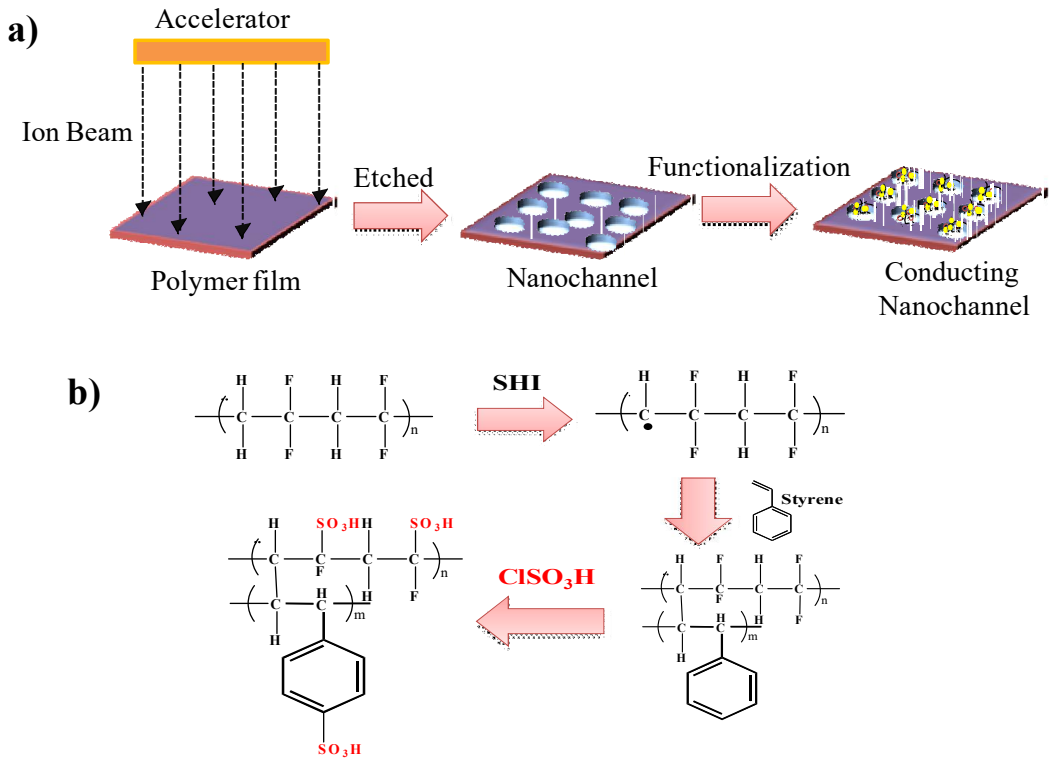

Figure 5.1: (a) Details schematic presentation of ion bombardment followed by their functionalization (physical representations); and **(b)** reaction scheme of the PVDF and nanohybrid grafting followed by the sulphonation (chemical representation).

Through nanochannels are clearly observed in etched specimens (right side images SEM of **Figure 5.2a**) both in pure PVDF and its nanohybrid as compared to irradiated specimens. The distribution of channel diameter indicates bigger size for pure PVDF (70±5 nm) against an average channel diameter of 40±3 nm in nanohybrid while the number density of the channels is higher in nanohybrid against pure PVDF (**Figure 5.2b**) . Uniformly distributed 2-D nanoclay in polymer matrix helps restricting the channel diameter in

nanohybrid. Similar channel formation with their relative dimension is also revealed through AFM images (**Figure 5.2 c&d**). This is worthy to mention here that size of irradiating ion, fluence (number of ions irradiated per unit area) and nature of matrix all together determine the size of latent track which eventually get reflected in nanochannel dimension after etching. This is to mention that nanoparticles help reducing the dimension of nanochannel while higher amount of nanoclay usually decrease the mechanical stability, a prime requirement for a membrane. Further, the free radicals in the side wall of the nanochannels are used up to carry out polymerization within the nanochannels for chemical tagging of the styrene monomer and its subsequent polymerization without any external initiator. Thus, variation in number density of channels and their size may help in different functionalization leading to alteration of membrane properties for their applications in various fields.

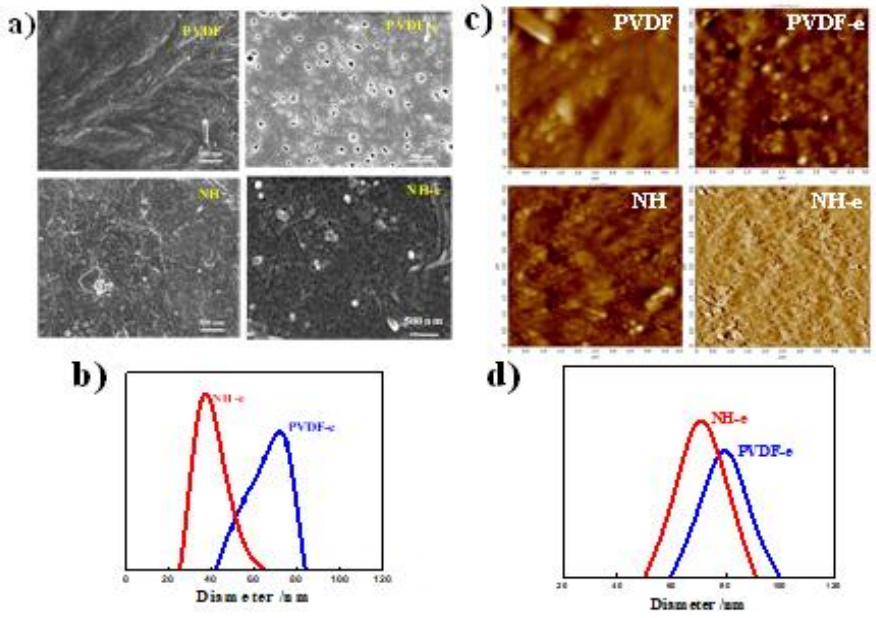

Figure 5.2:(a) SEM micrographs of PVDF, PVDF-e, NH and NH-e, showing tiny nanochannels after etching; **(b)** the distribution of nanochannel diameter of the etched membrane as observed in SEM images; **(c)** AFM micrographs of PVDF, PVDF-e, NH and NH-e, indicating nanochannels after etching; and **(d)** the distribution of nanochannel diameter of the etched membrane as observed in AFM images.

5.3.2 Functionalization of nanochannels:

Irradiation of swift heavy ions on the polymer matrix is known to produce reactive sites like free radicals, double bond, and ionic species in the polymer chains as the energy of the particle radiation is much higher as compared to carbon-carbon or carbon-hydrogen single bond energy, present in the back bone of polymer.[213] After the selective chemical etching, the free radicals are uncovered within the nanochannels and are being utilized to graft other polymer like polystyrene exclusively in the nanochannels through polymerization. [21] It should be mentioned here that some free radicals are also generated in the surface of the polymer film during irradiation which is oxidized in presence of air during storage of irradiated specimens while the free radicals were buried in the bulk of the film. So, the polymerization or grafting of polystyrene is performed immediately after etching experiment to avoid the oxidation of free radical within the nanochannel. The appearance of a new peak at (chemical shift δ=) 8.14 ppm is due to -SO_3H group of the polystyrene grafted PVDF/NH (both PVDF-g-s and NH-g-s) (**Figure 5.3a**). [21][60] Further, a new peak appears in the region of 7.71 ppm after grafting followed by sulphonation, apparently due to sulfonate group attached to backbone of polymer (both PVDF and NH) in addition to the peak at 2.35 and 2.84 ppm due to head to head (H-H) and head to tail (H-T) of PVDF chain, respectively. [98] Further, three new peaks appear at

6.97, 7.07 and 7.17 ppm both in PVDF-g-s and NH-g-s specimens is due to aromatic protons of polystyrene side chain along with two more new peaks at 1.90 and 4.24 ppm due to the aliphatic proton of styrene moieties after grafting (**Figure 5.3a**) [214]. Now from the Eq. (1), calculate the degree of the sulphonation (DS %) of the PVDF-g-s/ NH-g-s functionalized membrane, indicating higher degree of sulfonation for nanohybrid (NH-g-s) of 16% in contrast to PVDF-g-s (14%). Higher DS in nanohybrid is visualized from its greater number density of nanochannels which in turn increase the overall surface area of the side walls of nanochannel where grafting can occur. The tagging of styrene monomer/polymer with PVDF is also confirmed from the new FTIR intense bands at 1534 cm^{-1} assigned to the stretching frequency for aromatic rings of styrene unit both in PVDF-g-s and NH-g-s, while two new peaks at 1067 and 979 cm^{-1} correspond to the symmetric and asymmetric S=O stretching vibrations, respectively, which alternatively prove the sulfonation in the grafted membrane (**Figure 5.3b**). A broad peak at 3745 cm^{-1} confirmed the hydrophilic sulphonate group in both grafted and sulfonated PVDF / NH membranes as opposed to the absence of the above peaks in pristine PVDF and NH.[166] Further, the bands at 830 and 1268 cm^{-1} in NH indicate β/γ- and exclusively γ-crystalline phase, respectively, against the characteristic peak of predominant α-phase at 755 and 794 cm^{-1} in pristine PVDF (**Figure 5. 3b**) [215] [146][216]. The intensity of the β/γ and γ-crystalline peaks increase after grafting and sulfonation presumably due to orientation of the chain in the confined space within the nanochannel.[197] However, greater extent of grafting and sulfonation in nanohybrid as compared to pristine PVDF is noticed both from NMR and FTIR studies. Moreover, a broad band at 344 and 413 nm is observed in PVDF-g-s and NH-g-s, respectively, in UV-visible spectrum due to $n \rightarrow \pi^*$ transition of the sulphonate

group, while the broader absorption band for nanohybrid indicates its greater grafting and subsequent sulphonation vis-à-vis pristine PVDF (**Figure 5.3c**). This is to mention that pure polystyrene shows a peak at 260 nm [156] which merge with broad sulphonate peak both in PVDF-g-s or NH-g-s while the peak at 247 nm for NH is due to $\pi \rightarrow \pi^*$ transition of olefinic bond present in the organically modified nanoclay in nanohybrid against no absorption peak for pristine PVDF [19]. In brief, spectroscopic studies confirm the grafting and functionalization of the nanochannel which is supposed to cover the empty nanochannel with ion conductive polymer. The changeover of phases in presence of nanoclay has great implication especially utilizing the piezoelectric behavior for energy harvesting application as recently reported [215] [183] [197] Moreover, similar degree of electroactive phases are reported of 40 [215], 75 [183] and 79% [197] and thereby ~70% of electroactive phase in the present study is very suitable for the application of smart membrane.

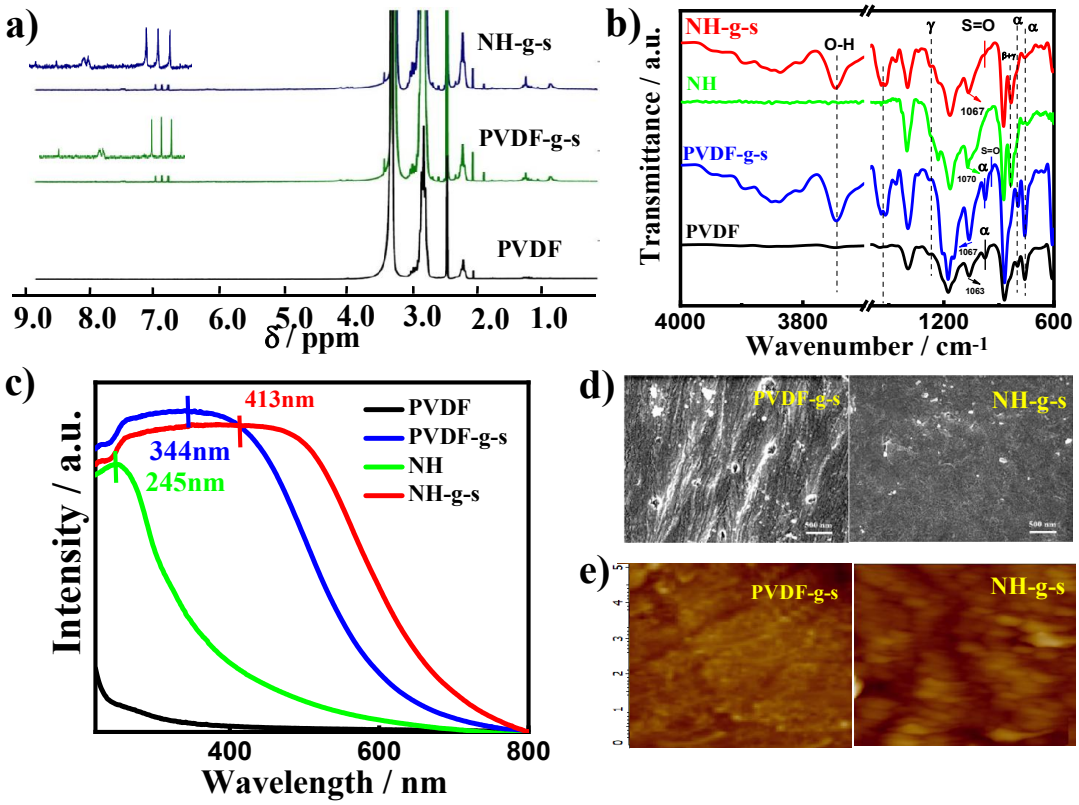

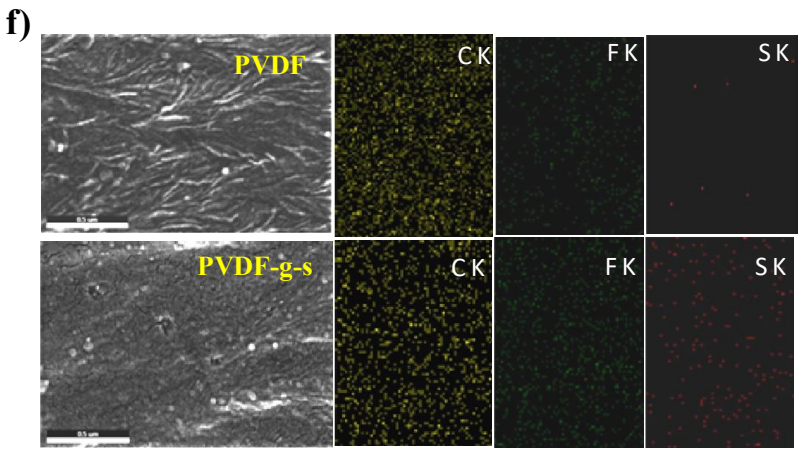

Figure 5.3: **(a)** Proton NMR spectra of PVDF, PVDF-g-s and NH-g-s with magnified spectra in the inset in the similar chemical shift; **(b)** FTIR spectra of PVDF, PVDF-g-s, NH and NH-g-s in ATR mode indicating the absorption peak and crystalline structural peak position; **(c)** UV –visible spectra of PVDF, NH, PVDF-g-s and NH-g-s indicating the peak position; **(d)** SEM images of PVDF- g-s, NH-g-s after the grafting followed by the sulphonation showing the cover up of the nanochannel due to grafting; **(e)** AFM images of the PVDF-g-s, NH-g-s after the grafting followed by the Functionalization indicating filing of the nanochannels after grafting, and **(f)** Energy-dispersive X-ray spectroscopy (EDS) and elemental mapping of PVDF; and PVDF-g-s (functionalize membrane) indicating the presence of sulphur after functionalization.

The coverage of the nanochannels using grafting followed by functionalization is explored through surface morphology. Both SEM (**Figure 5.3d**) and AFM images (**Figure 5.3e**) indicate the filled nanochannel originating from the grafting/functionalization of the channels exclusively (*cf.* **Figure 5.2a**). Further, the elemental mapping of the surface of the specimens through EDX clearly indicate the strong presence of sulphur after functionalization as opposed to the absence of sulphur before grafting and functionalization

(**Figure 5.3f**). However, the evidence of functionalization and grafting is proved through different spectroscopic techniques *e.g.* NMR, FTIR, UV-visible and energy dispersive X-ray spectroscopy (EDX) and functionalization process fulfill the nanochannels with ion conductive polymer and is expected to exhibit superior properties of a typical membrane including electrical transport phenomena and heavy metal removal from waste.

5.3.3 Functionalization induced structural change:

Figure 5.4a shows the wide angle X-ray diffraction patterns of PVDF, NH and their functionalized specimens. Pure PVDF exhibits different characteristic peaks of non-polar α-crystalline polymorph ($TGTG$) at 2θ = 17.6 ^{0}, 18.2 ^{0}, 19.8 ^{0} and 26.4^0 corresponding to (020), (110), (111) and (120) / (021) planes while nanoclay induces the polar crystalline β (TTTT) phase in nanohybrid at a 2θ value of 20.2^0 corresponding to (200/110) planes due to greater dipolar interaction between nanoclay and PVDF. [197], [217] ,[218], [219] Interestingly, β-peak intensity has enhanced after grafting followed by sulfonation within the nanochannels. The quantification of polar β-phase has been done through deconvolution of XRD spectra as shown in **Figure 5.4b** and a bar diagram indicates the presence of relative β-phase in different specimens (**Figure5.4c**). Considerably higher β-phase fraction is achieved in NH-g-s (64%) against 34% value of un-irradiated NH. Under similar Ag ion irradiation and functionalization generate meager 11 and 3% β-phases in PVDF-g-s and pure PVDF, respectively. This is to mention that polar β-phase is electroactive which exhibits piezoelectric properties, requirement of a smart membrane. Similar higher β-phase fraction has been reported by Tiwari et al. by making fiber of PVDF-nanohybrid for energy harvesting [197]. Higher β-phases in NH-g-s and PVDF-g-s are further substantiated from their melting behavior (**Figure 5.4d**). PVDF-g-s and NH-g-s

(after grafting and subsequent sulphonation) show the melting temperature of 161 and 160 ^{o}C, respectively, as opposed to the melting temperature of PVDF (175 ^{o}C) and NH (179 ^{o}C). The significant decrement of melting temperature is an indicative of the formation of low melting polar β-phase after grafting and functionalization process. [197][141] Greater decrement in NH-g-s is another signature of higher β-phase fraction vis-à-vis PVDF-g-s. Further, the heat of fusion (ΔH) reduces to 16.7 and 11.8 J/g for PVDF-g-s and NH-g-s from their respective values of 32.4 and 27.7 J/g for pure PVDF and NH. Interactions predominantly at the dipolar interfaces are mainly responsible for the reduction in heat of fusion in diluted system. Hence, the dipolar interaction between sulphonate group with the main chain of polymer is responsible for the considerable decrease of melting temperature along with heat of fusion in grafted and functionalized species.[216]

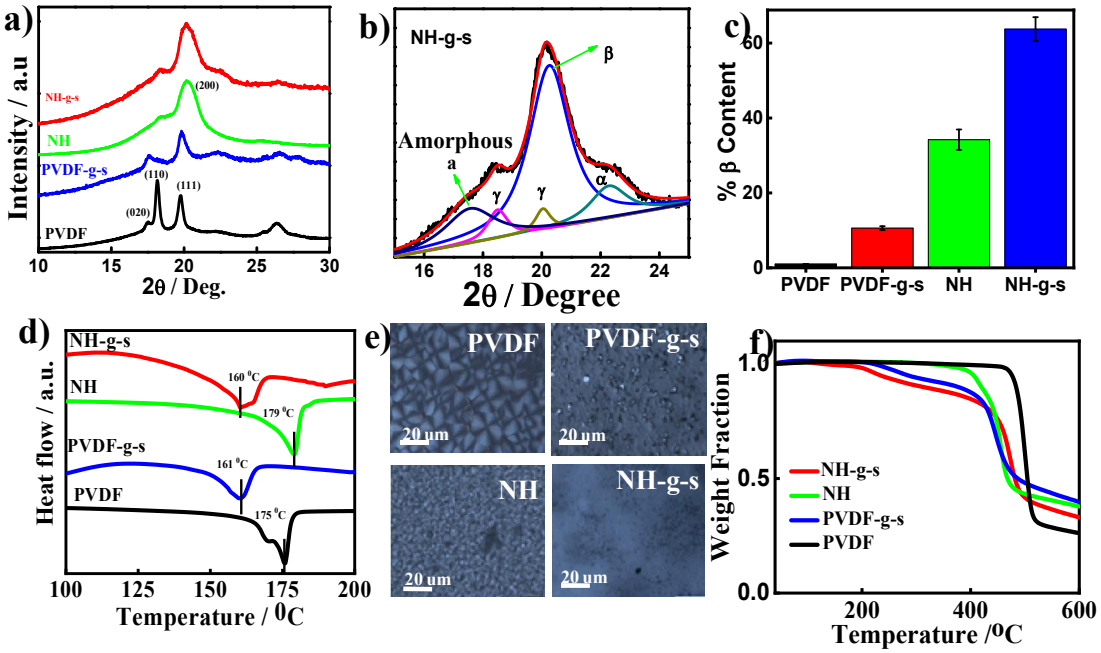

Figure 5.4: **(a)**XRD patterns of PVDF, PVDF-g-s, NH and NH-g-s membranes showing crystalline planes; **(b)**deconvolation of the functionalized nanohybrid membrane indicating various phases; **(c)** Bar diagram of piezoelectric β-phase content of PVDF, PVDF-g-s, NH and NH-g-s membranes;**(d)** DSC thermograms of the indicated specimens mentioning the melting temperature through vertical lines; **(e)** Polarizing optical microscopic images of PVDF, PVDF-g-s, NH and NH-g-s membranes showing spherulitic pattern in pure PVDF and mesh-like morphology in others; and**(f)** TGA thermograms of pure indicated specimens showing thermal stability of the membranes.

Compact spherulite is observed in pure PVDF under cross nicol polarized light which gets distorted after grafting and functionalization (**Figure 5.4e**). On the other hand, mesh like morphology is evident in nanohybrid due to induction of β-phase in presence of nanoclay in nanohybrid and a smooth morphology is evident after grafting and functionalization of NH is the indication of morphological induced structural change. However, the grafting and subsequent sulphonation also induce the phase conversion which alter the morphology of PVDF along with its structure. The thermal stability of the functionalized specimens is conducted through thermogravimetric measurement (weight loss as a function of temperature). The initial degradation temperatures are found to be at 281 and 226 ^{o}C for of PVDF-g-s and NH-g-s, respectively, due to the thermal degradation of sulphonate group while the main chain of the polymer degrades at much higher temperature (~450 ^{o}C), almost similar to the degradation of pristine PVDF (**Figure 5.4f**) [13]. The lowering of degradation temperature of the functionalized polymer is due to the insertion of the styrene and sulphonate (-SO_3H) group in the backbones of the PVDF chains. Further, the relatively lowering of degradation temperature in nanohybrid (NH-g-s)

is presumably due to greater extent of sulphonation as discussed earlier. However, the functionalized membranes are quite stable up to their respective melting temperature of ~160 ^{o}C and thereby suitable for real applications either in fuel cell membrane or heavy metal removal including waste radionuclides.

5.3.4 Electrochemical analysis and functionalized material as corrosion inhibitor:

It is necessary for a membrane to transport ionic species in order to act as fuel cell membrane or removal of heavy metal ions from the waste. To understand the proton conducting capability of the functionalized membrane, EIS (electrochemical impedance spectrometry) has been performed and the corresponding Nyquist plots of the functionalized membranes are shown in the **Figure 5.5a**, and measure the polarizing resistance using the fit and simulation method. The resistances of the functionalized membranes are found to be considerably low as compared to pristine PVDF (19.9Ω) or NH (17.6Ω) which is 2.19 Ω for NH-g-s and 6.96 Ω for PVDF-g-s. The proton conductivities, calculated from the polarizing resistance using Eq. (4), of the membranes are found to be very high for NH-g-s (0.13 S.m^{-1}) as compared to PVDF-g-s (0.048 S.m^{-1}) (**Figure 5.5b**). Higher proton conduction in functionalized nanohybrid is explained from greater degree of sulphonation in general and larger number density of conducting nanochannels in nanohybrid. Further, proton conduction increases systematically with increasing temperature maintaining the relative higher values for functionalized nanohybrid than that for PVDF (**Figure 5.5c**). At this juncture, it is important to mention that commercial membrane like standard Nafion shows lowering of proton conduction after 60 ^{o}C, **Figure 5.5c** raising thermal stability issue of the standard membrane, while steep increase of proton conductivity is observed for functionalized nanohybrid even at higher temperature

suggesting high temperature stability of the developed membrane. The higher proton conductivity of NH-g-s as compared to functionalized PVDF-g-s because of the organically modified two-dimensional silicate nanoclay addition as fillers reduces the hydrophilic channels in polymer matrix similar to the Nafion matrix from 6.5 to 7·9 nm, and thereby, facilitates proton conduction and inhibits the fuel cross over. [57] Hydrophilic ceramic/inorganic fillers, such as SiO_2, TiO_2, ZrO_2, zeolites are added to polymer matrix to retain water in the composite membrane at higher temperatures and high humidity makes them better performing fuel cell membrane. [56] These hydrophilic inorganic/organic materials, when incorporated with polymer matrix, increase the binding energy of water as well as the number and strength of active sites. The frequency dependence behavior of the membranes have been plotted in **Figure 5.5d** showing the modulus and phase angle as a function of frequency. The potentiodynamic polarization behavior (anodic and cathodic current-potential) (I-V) characteristics of representative concentration of functionalized membranes of PVDF-g-s and its nanohybrid (NH-g-s) are shown in **Figure 5.5e**. Blank coupon (mild Steel) is also explored and extrapolated up to their intersection point whose coordinates represent corrosion current (I_{corr}) and corrosion potential (E_{corr}) on the respective axes.[220][221] In case of NH-g-s, the corrosion current density decreased from 0.008954 $A.cm^{-2}$ (blank coupon) for inhibitor free solution to 0.00069 $A.cm^{-2}$ for 300 ppm of the inhibitor. The corresponding steady state corrosion potentials (E_{corr}) are found to be shifted from −0.435 to −0.469 V at the same concentration of inhibitor. Similar experiment is also performed in PVDF-g-s and found the current density of 0.0019 A/cm^2 and potential shifted -0.439 V as compared to the blank. Concentration variation of potentiodynamic polarization curves for other specimens (PVDF-g-s and NH-g-s) are shown in **Figure 5.5 f**

&g. The shift of cathodic polarization curves towards lower potential on successive addition of the inhibitor indicates the corrosion inhibition and the extent of corrosion inhibition are calculated from the **Eq. (6).** It is evident that the inhibition efficiency increases gradually with increasing concentration of the inhibitors. Interestingly, functionalized nanohybrid (NH-g-s) exhibits higher inhibition as compared to PVDF-g-s throughout the concentration window and 92% corrosion inhibition is achieved using 300 ppm of functionalized nanohybrid (NH-g-s) (**Figure 5.5h**). Similar results from the charge transfer resistance also suggest that the NH-g-s is more corrosion resistance than PVDF-g-s and better corrosion inhibition of functionalized nanohybrid lies in its higher degree of sulphonation which can transport easily under a potential and cover (or get electrodeposited) on the metal surface causing inhibition. To explore the surface coverage, optical images are taken after corrosion experiment which clearly indicates full surface coverage using NH-g-s against highly corroded blank and partially surface coverage using PVDF-g-s (**Figure 5.5i**). Hence, Tafel polarization plot and subsequent analysis clearly indicate the corrosion inhibition behavior of functionalized membranes. However, the electrochemical studies explored the high proton conduction of the functionalized nanohybrid along with its superior corrosion inhibition.

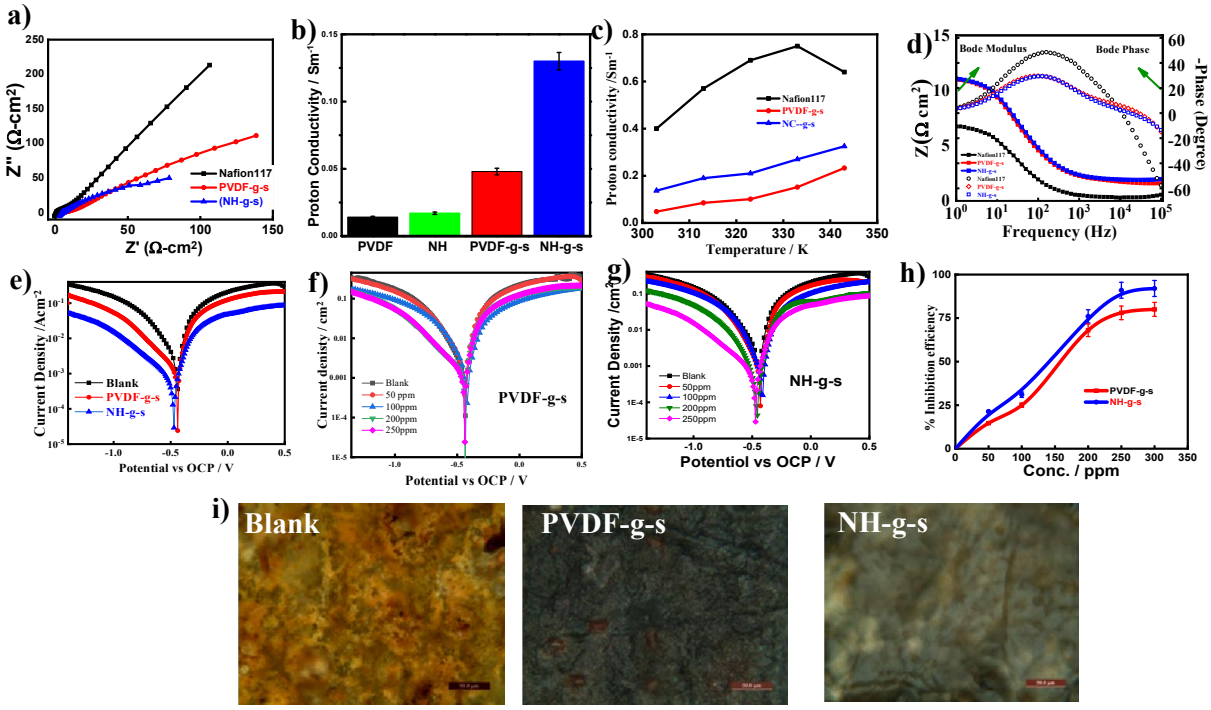

Figure 5.5: Electrochemical and potentiodynamic polarization studies of the membranes. **(a)** Nyquist plot of the indicated functionalized membranes (PVDF-g-s and NH-g-s); **(b)** Bar diagram showing the proton conductivity of the functionalized membrane (PVDF-g-s ,NH-g-s) at room temperature; **(c)** Proton conductivity of the functionalized membranes as a function of temperature; **(d)** Bode phase and modulus of PVDF-g-s ,NH-g-s membranes comparing Nafion117 as a function of frequency; **(e)** Tafel plot of blank, PVDF-g-s and NH–g-s at a concentration of 300 ppm; **(f)** Tafel plot of PVDF-g-s with concentration variation; **(g)** Tafel plot of NH-g-s with concentration variation;**(h)** Percentage inhibition using indicated species as a function of inhibitor concentration; and **(i)** surface coverage during corrosion experiment where complete surface coverage takes place using NH-g-s while partial and highly corroded surfaces are observed using PVDF-g-s and blank coupon, respectively.

5.3.5 Separation of radionuclide from waste and fundamentals:

Fabricated functionalized membranes having ion conducting nanochannels are explored for the sorption study of radionuclide ($_{241}Am^{+3}$ ions) present at trace level from the aqueous solution. Membranes were immersed in aqueous solution for the sorption of the radionuclide whose activity was measured from the using γ-emission at different times (**Figure 5.6a**). The sorption kinetics is higher for NH-g-s membrane as compared to PVDF-g-s throughout the measurement and attains a plateau after 2h which define the limit of sorption behavior using the particular membrane. **Figure 5.6b** compares the sorption capacity of membranes showing 80% removal of $_{241}Am^{+3}$ ions using NH-g-s membrane from the solution against ~70% using PVDF-g-s and the significantly higher value of absorption in nanohybrid membrane arises from its greater sulphonation as discussed above. Quantitatively, 0.358 μg.cm^{-2} (equivalent to 80.44 μg per gram of membrane) $_{241}Am^{+3}$ is adsorbed in NH-g-s membrane against 0.310 μg.cm-2 in PVDF-g-s. This is to mention that meager absorption takes place (~5% corresponding to 0.015 μg.cm-2) using pristine PVDF/NH films of similar dimension. Greater sorption in nanohybrid membrane (NH-g-s) vis-à-vis PVDF-g-s lies in its higher functionalization as discussed above. The radionuclide sorbed membranes were covered with C-39 detector for 5 min to register the track of alpha particles from $_{241}Am$ in C-39 detector. The radiographic images of the etched detector indicate the size of the track where radionuclides are absorbed (**Figure 5.6c**). The uniformity of the radiographic track also endorses the regularity of through nanochannels as observed through SEM/AFM. This is to mention that the absorption of radionuclides takes place through ion exchange mechanism (with -SO_3Na group present in the etched track) and the stability of $_{241}Am^{+3}$ ions occurs through complexation of $_{241}Am^{+3}$ ions with

the surroundings $-SO_3^-$ ions present in the constricted nanochannel/track. Adsorption of radionuclides may also a possibility but its extent is very less as evident from meager sorption in pure PVDF/NH. In this juncture, it is important to compare the sorption efficiency as reported in the literature. Glycidyl methacrylate monomer grafted on Teflon sheet showed meager efficiency of 0.25 μg/g [25] while functionalized microporous PES membrane after grafting of monomer HEMP and AMPS reported a moderate sorption efficiency [110] of 48.4 μg/g. This is to mention that the present work reports the sorption efficiency of 80.4 μg/g, significantly higher than the literature reported values. The reason behind the higher efficiency lies on the through nanochannels where overall surface area for ion exchange capacity is quite high as opposed to normal/microporous surfaces in the literature. The deloading experiment is carried out to understand the sequestering ability using different complexing agents such as HNO3, oxalic acid and EDTA and found 43, 47 and 50% of deloading, respectively, in PVDF-g-s while 37, 41 and 48% are noticed in NH-g-s membrane using same set of complexing agents **(Figure 5.6d).** Hence, EDTA is found to be a better complexing agent for $_{241}Am^{+3}$ ions and nanohybrid exhibits better retention power presumably due to greater constriction in smaller size nanochannel as compared to PVDF and schematic of the desorption shown in **Figure 5.6(e).**

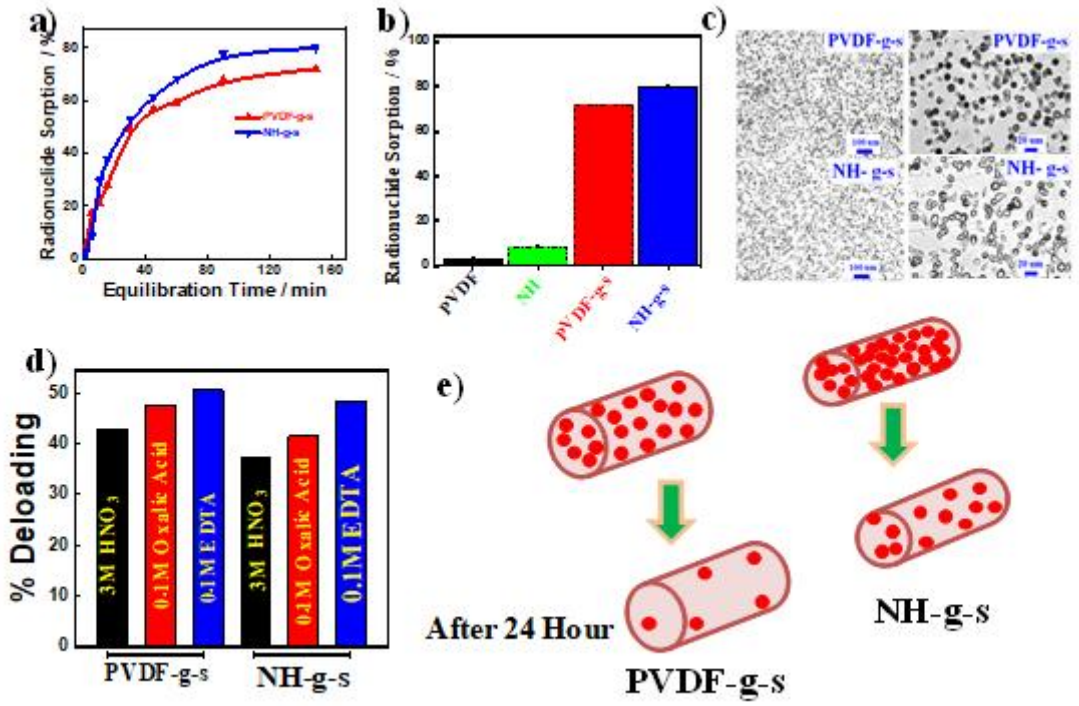

Figure 5.6: Radionuclide sorption experiments and radiation emission studies using functionalized nanochannel membrane. **(a)** kinetics of Am^{+3} sorption studies using indicated functionalized membranes (PVDF-g-s and NH-g-s); **(b)**Bar diagram showing maximum uptake efficiency of different functionalized membranes; **(c)** Radiographic images of the radioactive loaded different membranes on C-39 detector (right side images are higher magnification of the corresponding left side images); **(d)** Deloading of adsorbed Am^{+3} ion in different complexing agents; **(e)** Schematic of the desorption of functionalized PVDF-g-s comparing with the NH-g-s membrane.

5.3.6 Fuel cell performance using functionalized membranes:

Being efficient ion conductor, the functionalized membranes are expected to be suitable for fuel cell membrane. The proton conductivity and water uptake are the two important parameters for proton transport membrane of fuel cell application and higher values of proton conductivity and water uptake are preferable for an efficient proton exchange membrane. Proton conductivity of functionalized PVDF and its nanohybrid membranes are measured and are presented in **Figure 5.7a**. Nanohybrid membrane (NH-g-s) exhibits higher proton conductivity as compared to PVDF-g-s in the entire temperature range and proton conductivity systematically increases at higher temperature for the both the membranes. NH-g-s shows high value of conductivity 0.13 S.m-1 against 0.05 S.m-1 for PVDF-g-s and higher conduction is due to the greater sulphonate ions in nanohybrid membrane. Water uptake of PVDF-g-s and NH-g-s membrane is found to be 10 and 14%, respectively, much higher than the pristine PVDF/NH (**Figure 5.7b**). Further, the ion exchange capacities, measured from radioactive counts using Cs, of PVDF-g-s and NH-g-s are found to be 0.22 and 0.33 mmole/gram, respectively. Higher values of water uptake and IEC of NH-g-s membrane indicate for an effective membrane for direct methanol fuel cell applications. Usually transport of proton proceeds through two broad mechanisms; one of them is vehicle mechanism where proton is combined with the water molecule present in fuel and then diffuses through the membrane and second mechanism is Grotthous mechanism, in which the proton transports through hopping mechanism. However, higher proton conductivity in functionalized nanohybrid (NH-g-s) is believed to be due to frequently available sulfonate group inside the walls of nanochannel either through hopping or diffusion processes and make easier as compared to PVDF-g-s. The slope of

Arrhenius plot (**Figure 5.7a**) measures the activation energy (Ea) and lower value of NH-g-s (16.54 kJ mol^{-1}) as compared to PVDF-g-s (24.94 kJ mol^{-1}) indicate minimum energy requirement for proton transport which eventually help achieving easier proton transport phenomena in nanohybrid membrane. This is to mention that much lower value in Nafion (10.05 kJ mol^{-1}) though help in proton conduction but high temperature stability becomes an issue. [19]

In order to understand the efficacy of the membrane, fuel cell has been fabricated following the membrane electrode assembly (MEA) as shown in **Figure 5.7c** using the flexible and mechanically strong membranes (**Figure 5.7d**) , Fuel cell performance of the functionalized membrane is examined through current–voltage polarization curves in direct methanol fuel cell (DMFC) as shown in **Figure 5.7e**. DMFC performance using functionalized nanohybrid membrane (NH-g-s) exhibits the slowest decay of the potential with increase of load with higher open circuit voltage (OCV) of 0.381 V vis-à-vis 0.30 V using PVDF-g-s membrane. Standard Nafion though exhibit higher OCV (0.60 V) but a relatively sharp decrease potential is noticed under load. Moreover, significantly higher power density is observed in NH-g-s (45 mW/cm^2) against 18 mW/cm^2 for PVDF-g-s at current density of 298 and 145 mA/cm^2, respectively (**Figure 5.7f**). Significantly higher output (power density) is observed for functionalized nanohybrid membrane as compared to standard Nafion (27 mW/cm^2) indicating superior power generation in fuel using the developed functionalized nanohybrid membrane. This is to mention that similar output of ~30 mW/cm2 is reported in literature for Nafion in its dry condition, which is very close to our measured values (27 mW/cm^2) while the increase of humidity in presence of hydrophilic filler enhances power output drastically. [56] In another work Sahu et al. [160]

developed new catalyst based on CNF having hetero atoms which exhibit power density of ~ 65 mW/cm^2. Nanofluids are considered as potential materials where better heat dissipation can be correlated with higher performance of a fuel cell and, thereby, increasing its conversion efficiency. The remarkable advancement in thermal engineering of a fuel cell cooling system mainly depends on nanofluid technology. Nanofluids prepared by dispersing nanocrystalline platinum anchored carbon nanotubes (CNTs) in water exhibit power density and current density of 0.35 mW/cm^2, 0.20 mA/cm^2, respectively . [155] Similarly Nafion filter membrane of 220 nm size act as nanochannel for microbial fuel cell with power density and current density of 0.08 mW/cm^2 and 0.06 mA/cm^2. [127] In comparison this work reports the power density and current density of 45 mW/cm^2, 298 mA/cm^2 using nanochannels created on PVDF nanohybrid after irradiating in an accelerator with silver ions. However, the high current as well as power density of functionalized nanohybrid membranes, prepared through Functionalization of accelerator irradiated hybrid membrane, are visualized from the high proton conduction using ionomer membrane.[213] The excellent fuel cell performance of functionalized nanohybrid membrane against to the std. Nafion117 and PVDF-g-s is mainly due to enhanced degree of sulfonation in presence of 2-D layered silicate uniformly dispersed in the polymer matrix. New functionalized membrane along with its electroactive piezo phase demonstrates the new generation smart fuel cell membrane using common thermoplastics like PVDF.

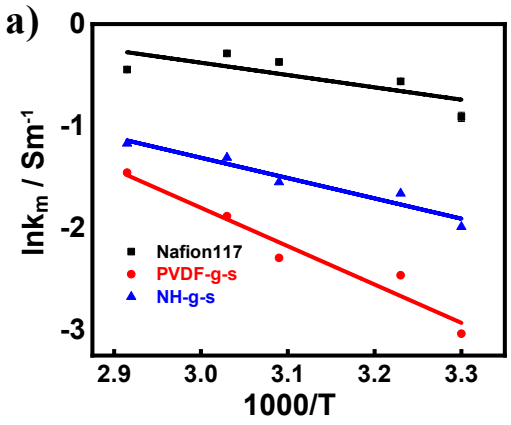

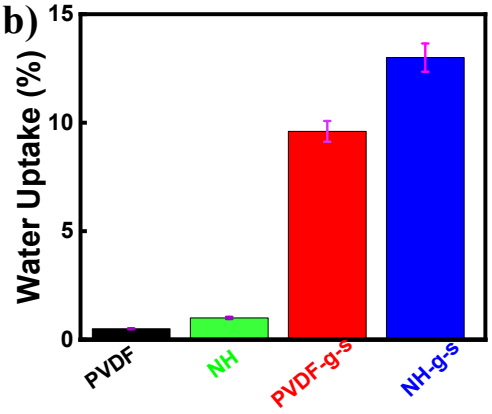

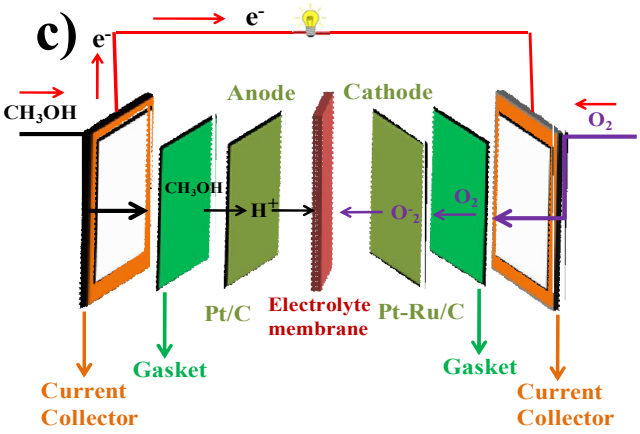

Schematic of Single Fuel cell Stack

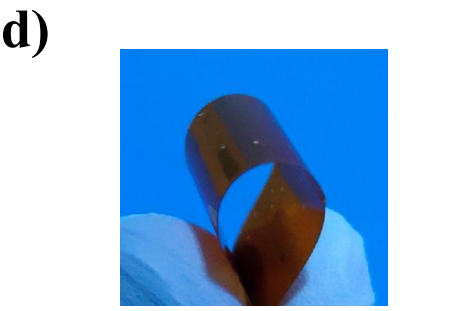

Functionalized membrane

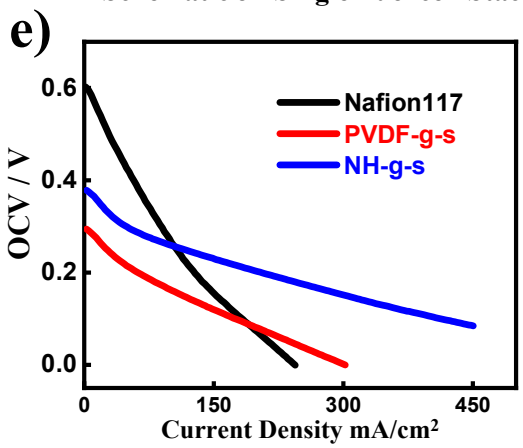

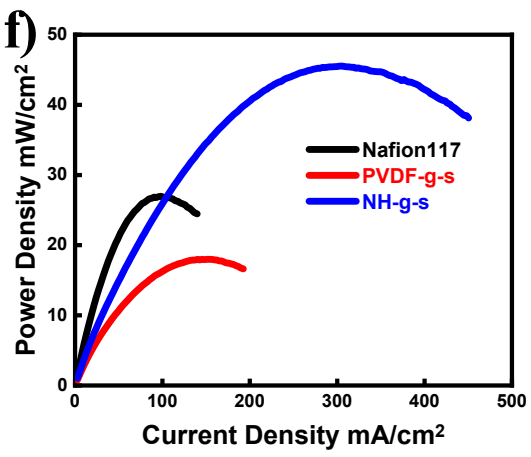

Figure 5.7: Complete fuel cell experiment using the developed membranes. **(a)** Proton conductivity of the indicated membranes as function of temperature; **(b)** water uptake of the functionalized membranes (PVDF, PVDF-g-s, NH, and NH-g-s); **(c)** Schematic presentation of membrane electrode assembly using developed membranes; **(d)** Photograph of representative functionalized membrane showing its mechanical stability along with flexibility; **(e)** Polarization curves of PVDF-g-s and NH-g-s membranes comparing standard Nafion and open circuit voltage; and **(f)** Fuel cell performance in terms of power density as a function of current density using the functionalized membranes and comparison with standard Nafion.

5.4 Conclusions

Predominantly amorphous latent tracks have been generated in polymer films using swift heavy ions bombardment. Nanochannels are created through selective chemical etching of the amorphous track. The dimension of nanochannel is controlled (40 nm) in nanohybrid in presence of dispersed two-dimensional nanoclay in PVDF matrix vs. 70 nm in pure PVDF. The nanochannels are grafted, utilizing the free radicals generated during SHI irradiation, using styrene monomer followed by sulphonation of the nanochannel exclusively to convert the nanochannels ion conducting. The proof of grafting and functionalization is visualized through a series of spectroscopic measurement like NMR, FTIR, UV-vis and EDX along with the filled surface morphology using SEM and AFM. Nanoclay and functionalization induce the piezoelectric phase as evident from X-ray diffraction patterns and lowering of melting endotherms in DSC thermographs as compared to pristine PVDF or its nanohybrid. Higher proton conduction (0.13 $S.m^{-1}$) through nanohybrid membrane is understood from it greater functionalization which helps hooping of proton across the

membrane under an electric field. The functionalized membranes act as good corrosion inhibitor and a very high inhibition efficiency (92%) is observed using nanohybrid membrane vis-à-vis pure PVDF (81%). The functionalized membranes effectively separate out the radionuclide from their solution/waste (~80% or 0.35 $\mu g.cm^{-2}$ or 80.44 μg/g of the membrane) using nanohybrid membrane. The absorption of radionuclide exclusively within the nanochannel is understood from radiographic image. Ion exchange capacity of the nanohybrid membrane is found to be 0.33 mmol/g which is comparatively higher than that of functionalized PVDF membrane (0.22 mmole/g) and thereby suitable for fuel cell application together with its high water uptake value (~13%). Membrane electrode assembly has been performed and fuel cell is designed using the functionalized membranes which demonstrate a high power generation capacity (power density) of 18 and 45 mW/cm^2 for PVDF and nanohybrid based membranes. Moreover, higher activation energy of nanohybrid membrane (16.5 kJ /mole) also reflects its high temperature stability as compared to standard membrane and, therefore, found multiple uses of the membrane designed through the approach mentioned.